

## Rheology of Entangled Solutions of Ring–Linear DNA Blends

Dejie Kong, Sourya Banik, Michael J. San Francisco, Megan Lee, Rae M. Robertson Anderson, Charles M. Schroeder, and Gregory B. McKenna\*

Cite This: <https://doi.org/10.1021/acs.macromol.1c01672>

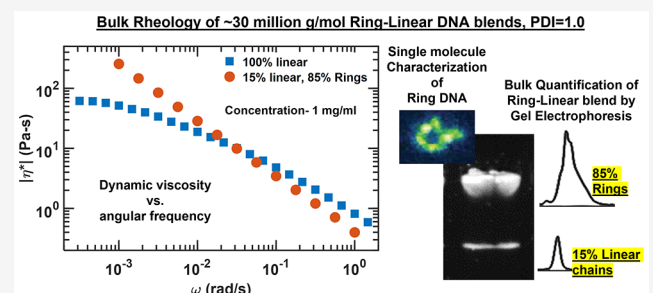
Read Online

ACCESS |

Metrics &amp; More

Article Recommendations

**ABSTRACT:** Bulk rheology measurements on concentrated monodisperse ring–linear DNA mixtures are reported for the first time. The entanglement behavior of the ring–linear DNA mixtures (with 15 and 50% linear chain fractions,  $\phi_{\text{Lin}}$ ) over a range of total DNA concentration,  $\phi_{\text{Tot}}$  from  $\sim 0.8$  mg/mL ( $20C^*$ ) to 2 mg/mL ( $50C^*$ ) is reported. A discussion on the current problems in the reported ring dynamics/scaling is included. The concentration-dependent dynamics of the ring–linear DNA mixtures are compared with the dynamics of 100% linear DNA at the same linear chain degree of entanglement,  $Z$ . Dynamic oscillatory tests were conducted to understand the bulk rheological behavior of the ring–linear DNA blends. The blends showed a broadening of the rubbery plateau region compared with that of the pure linear counterparts—not reported in any previous works on ring polymers. However, the final plateau moduli,  $G_N^0$ , of the ring–linear mixtures were found to be lower than for the pure linear DNA at the same total concentration. The plateau moduli for the mixtures followed a 2.2–2.3 power law dependence with total concentration,  $\phi_{\text{Tot}}$  similar to the scaling seen in the 100% linear analogue.  $G_N^0$  for the blends scaled as  $G_N^0 \sim (\phi_{\text{Tot}})^{2.2-2.29} (\phi_{\text{Lin}})^{0.7-0.8}$  for the two linear chain percentages and the range of concentrations studied. The blends at the same total concentration exhibited much higher viscosities relative to the linear counterparts than reported by prior works on synthetic ring melt systems. This is consistent with very long terminal relaxation times most likely due to linear chain threading of these very large macromolecules. The zero shear viscosities for the blends with only 15% linear chain fraction could not be obtained at shear rates as low as  $10^{-5} \text{ s}^{-1}$ . The Cox–Merz rule was found to hold for the ring–linear blends. Linear chains seem to dictate the dynamics and the entanglement scaling of the blends even at low linear chain fraction of 15%.



## 1. INTRODUCTION

Synthetic ring polymers and their dynamics have been studied for several decades both in the melt and in dilute solution. The circular topology has piqued interest as the absence of free chain ends poses topological constraints which obviates reptation dynamics and consequently the possible mechanisms of entanglement and scaling laws.<sup>1,2</sup>

The earliest ring polymer syntheses were reported by Semlyn<sup>3,4</sup> for polydimethylsiloxane (PDMS), Rempp and co-workers<sup>5,6</sup> and Geiser and Hocker<sup>7</sup> for polystyrenes (PS), and Roovers and Toporowski<sup>8,9</sup> for polybutadienes (PBD) and polystyrenes. The early synthesized and studied “pure” rings initially thought to be devoid of linear chains have now been established to have significant linear chain contamination.<sup>8–15</sup> Moreover, high molecular weight rings free of linear chains were not successfully synthesized with the early ring closure polymerization (RCP) technique. The ring PDMS synthesized by ring–chain equilibration reaction of siloxane oligomers also did not give high molecular weight polymers. Hence, the nominal entanglement dynamics of pure rings having high entanglement densities was not successfully studied. A more recent synthesis technique, the ring-opening metathesis

polymerization (ROMP),<sup>10,16</sup> can make fairly large rings. This method might still have the linear contamination issues due to side reactions during the ring-opening that can lead to large amounts of linear chains and other undesirable topologies like double rings. Also, their entangled rheology has not been reported. Molnar et al.<sup>17</sup> have reported large polyisobutylene (PIB) and poly(3,6-dioxo-1,8-octanedithiol) (polyDODT) rings synthesized by a redox radical recombination polymerization (R3P) reaction,<sup>18</sup> but these have not yet been shown to have <6% linear chain contamination. New chromatographic techniques of fractionating pure rings have been put forward, and the samples have been touted as “pure”.<sup>19,20</sup> Several of these treatises reported no development of an entanglement plateau in the time-dependent behavior of the viscoelastic moduli of the ring samples.<sup>13,14</sup> But further analysis of the rheological data

Received: August 7, 2021

Revised: January 15, 2022

shows inconsistencies such as an unexpectedly high molecular weight dependence of the viscosities of some of these rings,<sup>13,21</sup> while others seem to show a linear dependence.<sup>14,22</sup> The current problems on the reported synthetic ring data are described in the next section.

Because of the inability of the community to (i) synthesize pure ring polymers of high molecular weight, (ii) difficulty in fractionating the ring/linear mixtures, (iii) lack of reliability in accurate characterization of the synthesized rings, and (iv) inconsistency in the reported data, we switch our efforts to investigate the entanglement of ring polymers by employing natural circular polymers, e.g., bacterial plasmid DNA. DNA offers the opportunity to make quantitative measurements of the level of contamination (through gel electrophoresis), and the large size of the molecules lets one study the entanglement behavior in low concentration solutions, thus partially overcoming the difficulty of making large quantities of DNA. Also, unlike the prior studies on bulk rheology of blends of linear and circular molecules, the DNA studied here is monodisperse in that the rings and linear contaminants have the same molecular weights (evidenced in the gel electrophoresis) rather than a mixture of nearly the same size<sup>12</sup> or mixtures of polydisperse rings with polydisperse linear chains<sup>23,24</sup> that may or may not be of the same size. Because of the ubiquitous problem and the continuing debate related to linear chain contamination, it is paramount to better understand the effects of blending of linear chains with the rings. Here, we report the dynamics of DNA systems of very large rings and linear chains in a controlled entanglement concentration and compare them with the behavior of a system of 100% linear chains of virtually the same molecular weight over a range of concentrations that would be lightly entangled to a highly entangled state.

**1.1. Current Problems with the Reported Ring Dynamics.** The early investigations by McKenna and co-workers<sup>11,25</sup> on polystyrene (PS) and Roovers and co-workers<sup>8,15,26–28</sup> on polystyrene (PS) and polybutadiene (PBD) rings showed a lower plateau modulus,  $G_N^0$ , and a higher steady-state recoverable compliance,  $J_S$ , for the rings when compared to their linear counterparts. The rings also showed a lower viscosity than the linear chains with some differences in the viscosity–molecular weight dependence. These ring samples are now known to have had significant linear chain contaminations up to tens of percent.<sup>15</sup>

Kapnistos et al.<sup>13</sup> reported high purity after fractionating the Roovers' rings with liquid chromatography at the critical condition (LCCC) method. The authors acquired rings at two different molecular weights, 161000 and 198000 g/mol. In their tests, the relaxation modulus did not show any development of a rubbery plateau and exhibited a power law relaxation. Kapnistos et al.<sup>13</sup> also tested adding linear chains to their pure rings. They showed a significant change in the observed linear viscoelastic (LVE) of the rings by adding a very low concentration of linear chains of 0.0007 g/cm<sup>3</sup> and concluded that they had rings “as pure as currently possible”. Although the LCCC remains the best method, recently Molnar et al.<sup>17</sup> questioned the sensitivity of the LCCC method and suggested that it is incapable of measuring <6 wt % linear contamination. More studies are needed to confirm the findings of Molnar et al.<sup>17</sup> Further work from the Greek group on the same “purified” polystyrene rings was conducted by Pasquino et al.,<sup>21</sup> who also reported the dynamics on poly(ethylene oxide) (PEO) and polyisoprene (PI) rings. In a separate work, the Japanese group synthesized PS rings from 10000 to 240000 kg/mol as reported by Doi et al.<sup>14</sup>

The authors also showed a relaxation without any development of a rubbery plateau in their dynamic measurements. A comparison of the viscosity dependence on molecular weight of polystyrene rings studied by different groups was reported by Doi et al.<sup>14</sup> at a reference temperature of 160 °C. Kapnistos et al.<sup>13</sup> and Doi et al.<sup>14</sup> are seminal works as both the articles did not show any entanglement plateau until  $Z \sim 12$  ( $Z$  being calculated assuming all linear chains), thus showing no entanglement effects in comparison to their linear counterparts. However, the entanglement molecular weight of the rings is not known, and whether the rings in these works were truly well entangled or not is questionable. Moreover, there are several inconsistencies in the reported data and differences in the scaling obtained. We discuss those in the next paragraph and in Figure 1.

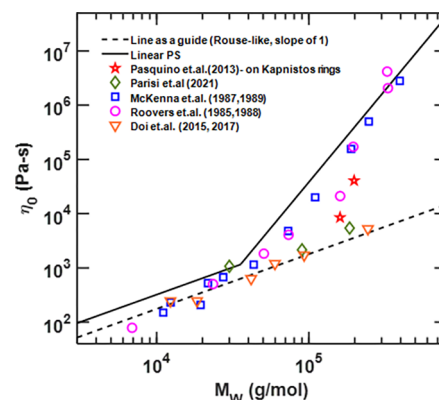


**Figure 1.** Molecular weight dependence of viscosity of synthetic polystyrene rings from different studies. All the data are at a reference temperature of 160 °C. ( $\nabla$ ) Doi et al.<sup>14,22</sup> and data presented at the 2017 conference “Ring Polymers: Advances and Perspectives”, Crete, Greece (unpublished data);<sup>29</sup> ( $\circ$ ) Roovers et al.;<sup>26,28</sup> ( $\square$ ) McKenna et al.;<sup>11,25</sup> ( $\star$ ) Kapnistos et al.;<sup>21</sup> ( $\diamond$ ) Parisi et al.<sup>28</sup> The dashed line with a slope of 1 (Rouse-like relaxation) is a guide for the eye for the ring samples. The thick bold line is for linear polystyrene melt behavior<sup>11,14,26</sup> showing the 1.0–3.4 dependence on molecular weight also acting as a guide for the eye.

In Figure 1, we show a comparison of the viscosity dependence on molecular weight of the synthetic polystyrene ring melts over a range of molecular weights as reported by different groups. To understand the scaling of the PS rings, the viscosity of linear PS is also shown in Figure 1. As observed, the contaminated PS rings studied by McKenna et al.<sup>11</sup> and Roovers<sup>26</sup> exhibit Rouse-like ( $\eta_0 \sim M^{1.0}$ ) to entangled ( $\eta_0 \sim M^{3.4}$ ) scaling similar to linear PS, and then  $\eta_0$  increases to very high scaling of ( $\eta_0 \sim M^{>5.0}$ ) at higher molecular weights. An analysis of the Kapnistos' purified ring data shown in Figure 1 shows a very high dependence of 7.5 power, i.e.,  $\eta_0 \sim M^{7.5}$ . The scaling exponent is much greater than the  $\eta_0 \sim M^{3.4}$  observed for entangled linear chains. The viscosity scaling is also consistent with the relaxation time scaling extracted from the relaxation curves in Kapnistos et al.<sup>13</sup> We acknowledge that presumably the data has its error bars, and the reliability of the fit (and the scaling obtained) here can be questioned as there are only two data points separated by a factor of  $\sim 1.2$  in molecular weight. However, the viscosity of the Kapnistos rings also have a greater magnitude than reported by Doi et al.<sup>14</sup> at the same molecular weights (Figure 1). This shows that the Doi rings possibly had a greater sample purity than Kapnistos rings. This was also suggested by Doi et al.,<sup>14,22</sup> and the authors proposed that the

Kapnistos rings might have  $\sim 5\%$  linear chain contamination. If the Kapnistos rings indeed had linear chains up to several percentages, it is perplexing that the samples still showed a significant change on adding 0.07 wt % linear chains. More importantly, both contaminated Doi rings and Kapnistos rings did not show any development of plateau in their LVE, but the Kapnistos data exhibited a higher viscosity scaling.

The originally reported data by Doi et al.<sup>14</sup> are also confounding because in the low molecular weight region the ring viscosities closely follow a Rouse-like behavior. In this region, the Doi data match with data from McKenna et al.<sup>11</sup> and Roovers<sup>26</sup> which are now thought to have contained linear chain impurities.<sup>15</sup> In the 2015 Doi et al.<sup>14</sup> paper, the highest molecular weight sample of 240000 g/mol followed a viscosity dependence of 2.4 power on molecular weight (data not shown in Figure 1) with a possible critical entanglement molecular weight,  $M_C$ , of  $\sim 90000$  (5 times that for linear chains). However, Doi and co-workers corrected the results in their next published article as they found that their highest molecular weight sample had 4–5% linear contamination.<sup>22</sup> In their 2017 paper they showed how an increase in the linear chain weight fraction in the samples increases the terminal relaxation response. In addition, the molecular weight dependence of viscosity on adding linear chains to a ring sample was presented in the 2017 conference, “Ring Polymers: Advances and Perspectives” in Crete, Greece (unpublished data)<sup>29</sup> by Y. Doi. A very striking observation is that, following the correction, the 240000  $M_w$  sample considered to be pure continued on the line from the lower molecular weight samples having a first power dependence ( $\eta_0 \sim M^{1.0}$ ) of viscosity on molecular weight, i.e., the same as what is seen in unentangled rings (possibly contaminated) and unentangled linear Rouse chains. The unusual scaling cannot be readily explained as dynamics of pure rings within our current understanding. The experimentally observed scaling is quite different from predicted scalings of 1.33–1.67<sup>30,31</sup> and 1.4<sup>32</sup> and 1.7<sup>33</sup> from molecular dynamics simulations and theoretical models such as the lattice animal model<sup>31</sup> and the fractal loopy globule model.<sup>34</sup> Although it can be argued that the experimentally observed  $\sim 1$  power scaling is close to 1.4 (scaling from simulations) due to experimental uncertainty, it cannot be confirmed to be true due to the reasons stated above and since the entanglement molecular weight of the pure rings is not known yet.

We suspect the treatises reporting very high viscosity scaling on molecular weight still have various but significant amounts of linear chain contamination in the studied ring samples which were not perfectly fractionated. However, the viscoelastic moduli from the rheological tests did not show any entanglement plateau. Furthermore, the LCCC fractionated ring PS samples showed a large change in the rheological response upon adding trace amounts of linear chains. The possibility of the final ring samples having other undesirable products like knotted rings also cannot be ruled out.<sup>15,35–37</sup> Knotted rings have been showed to have close but smaller radii of gyration than rings. Also, there is a possibility of having different types of knotted topologies present in the sample.<sup>35,36</sup> We do not know the effect of knotted structures on entanglement and dynamic behavior nor do we know the effectiveness of the current fractionation steps to remove such species. Several of the authors of these articles have discussed the possibility of varying purity in the fractionated ring samples.<sup>22–24</sup> Opening up of the rings on thermal treatment or shear on multipass procedures which may introduce linear

chains is another problem that might affect the relaxation behavior. Clearly sample purity and its reliable characterization are paramount in observing the pure ring behavior.

The previous paragraphs in this section have been included to show that there is considerable uncertainty in the reported dynamics of the synthetic rings and, especially, in the molecular weight dependence of the viscosity. Sample purity and linear chain contamination remain significant problems, and the true behavior of pure rings is still unknown. Regardless, the previously mentioned articles are significant as they provide several important rheological features of rings and ring–linear blends. We emphasize that synthesis of large polymer rings and fractionating/removing linear chains to get very pure rings is intricate, and the endeavors are plagued by extremely limited samples. Clearly, purification of ring samples and avoiding linear chain contamination is a far greater problem than previously thought.

McKenna and Plazek<sup>12</sup> were the first to look at the possible effects of linear chain contamination on the viscoelastic response of polystyrene rings, and their results were confirmed by Roovers,<sup>28</sup> who looked at a wider range of linear chain concentrations in a polybutadiene system. To understand the effect of linear chain contamination on rings, Roovers<sup>28</sup> plotted the viscosity of ring–linear blends normalized with 100% linear chain viscosity against linear chain fraction. He found that the scaled viscosity goes through a maximum at  $\sim 50\%$  linear chain concentration. The plot also shows a dramatic increase in the normalized viscosity with increase in linear chain concentration from a nominal 0% to 20%. On plotting the Kapnistos data (from Pasquino et al.<sup>21</sup>) and Doi’s data<sup>14</sup> along with that of Roovers on the same plot, it can be seen in Figure 2 that the Kapnistos data follow closely Roovers’ data, indicating that both

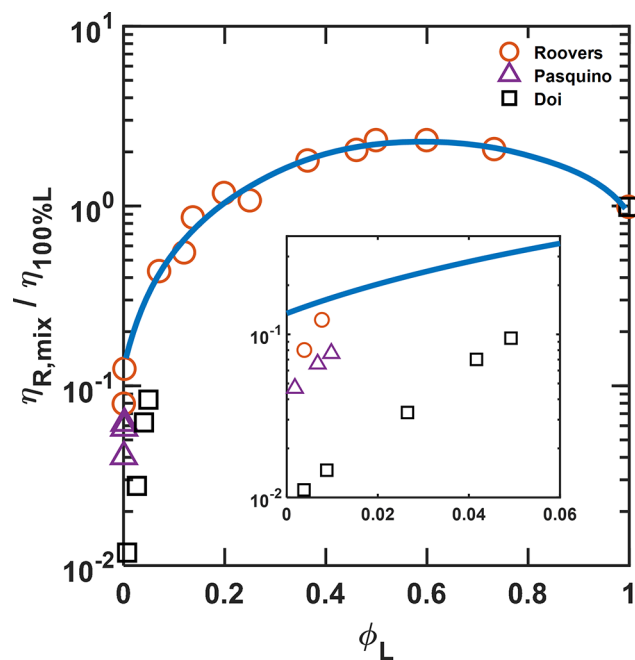


**Figure 2.** Comparison of linear chain addition effects on viscosity of circular polymers from different works. Plot of ring–linear mixture viscosity normalized by the viscosity of the linear melt as a function of the mass fraction of linear chains in the mixture. Data from Roovers<sup>26,28</sup> include results for both polystyrene and polybutadiene rings. The line is a guide to the eye to Roovers’ data. The inset shows an enlarged view of the data at low linear chain fraction.

**Table 1. Samples Used in This Work, Their Ring–Linear Composition in Percentage, and Total Concentration**

| samples                    | linear chain (in mass fraction), $\phi_{Lin}$ | total concentration, $\phi_{Tot}$ (mg/mL) |                     |                     |
|----------------------------|---|---|---------------------|---------------------|
| ring–linear blend (fosmid) | 0.15 $\pm$ 0.02                               | 0.84 $\pm$ 0.05 (0.8)                     | 1.08 $\pm$ 0.05 (1) | 1.96 $\pm$ 0.07 (2) |
| ring–linear blend (fosmid) | 0.50 $\pm$ 0.02                               | 0.80 $\pm$ 0.05 (0.8)                     |                     | 2.10 $\pm$ 0.07 (2) |
| 100% linear ( $\lambda$ )  | 1.00  | 0.82 $\pm$ 0.05 (0.8)                     | 1.01 $\pm$ 0.05 (1) | 2.06 $\pm$ 0.07 (2) |

**Table 2. Ring and Linear DNA Strains Used, Size/Molecular Weight, Radii of Gyration, Overlap Concentration, Entanglement Concentration, and the Number of Entanglements at a Total Concentration of 1 mg/mL**

| sample                          | size (kbp)/mol wt, $M_w$ (g/mol) | radius of gyration, $R_g$ ( $\mu$ m) | overlap conc $\phi^*$ (mg/mL) | entglmnt conc $\phi_e$ (mg/mL) | number of entanglements/chains, $Z$ calculated by different methods listed in Banik et al. <sup>40</sup> assuming linear chain topology (see text for meaning of $Z$ ) |                                      |                                      |
|---------------------------------|----------------------------------|--------------------------------------|-------------------------------|--------------------------------|--|--------------------------------------|--------------------------------------|
|                                 |                                  |                                      |                               |                                | $\phi_{Tot} = 0.8$ mg/mL   | $\phi_{Tot} = 1$ mg/mL               | $\phi_{Tot} = 2$ mg/mL               |
| <b>circular</b><br>FOS45<br>DNA | 45/                              | $R_{g,L} = 0.64$                     | 0.044                         | 0.396                          | $(\phi_e = 9\phi^*)$<br>$Z \sim 2.6$   | $(\phi_e = 9\phi^*)$<br>$Z \sim 3.4$ | $(\phi_e = 9\phi^*)$<br>$Z \sim 8.4$ |
|                                 | $2.9 \times 10^7$                | $R_{g,C} = 0.41$                     | 0.168                         |                                | $(\phi_e = 4\phi^*)$<br>$Z \sim 7.3$   | $(\phi_e = 4\phi^*)$<br>$Z \sim 9.4$ | $(\phi_e = 4\phi^*)$<br>$Z \sim 23$  |
|                                 |                                  |                                      |                               |                                | $(c_v = 1)$<br>$Z \sim 15$   | $(c_v = 1)$<br>$Z \sim 21$           | $(c_v = 1)$<br>$Z \sim 61$           |
| <b>linear</b><br>$\lambda$ DNA  | 48.5/                            | $R_g = 0.67$                         | 0.042                         | 0.376                          | $(c_v = 10)$<br>$Z \sim 25$  | $(c_v = 10)$<br>$Z \sim 34$          | $(c_v = 10)$<br>$Z \sim 107$         |
|                                 | $3.15 \times 10^7$               |                                      |                               |                                |  |                                      |                                      |

the Kapnistos and Roovers rings might have similar amounts of linear chain contaminant, possibly up to several percent. However, the Doi data fall below the other two data sets, which is consistent with a lower linear chain contamination in their rings.

The impact of linear chains on the viscoelastic response of rings is significant. This problem is even magnified as we suspect the minimum concentration of linear chains at which their effects on the dynamics would disappear may be as low as a fraction of a percent. Indeed, the single molecule dynamics of ring DNA in a linear DNA background suggests that the effects of linear chain contamination could be observed at concentrations as low as  $0.025\phi^*$  where  $\phi^*$  is the overlap concentration.<sup>39</sup>

Hence, studying the viscoelastic behavior of linear chains in mixtures of rings and linear chains is important to determine how the presence of small amounts of linear chain contamination affects the pure ring dynamics.

## 2. EXPERIMENTAL SECTION

**2.1. Materials and Essential Parameters.** The ring/ring–linear blend sample was chosen to be a 45 kilobase pair (kbp) ( $2.92 \times 10^7$  g/mol) DNA fosmid strain. The fosmid DNA (aka FOS45) is a bacterial plasmid with an artificial construct from *E. coli*. It has a unique restriction site and antibiotic resistance termed as pCC1FOS45 in which pCC1FOS is the vector containing the oriV origin. In a ring–linear blend sample with 15% linear chain percentage there is 15% mass fraction of 45 kbp linear chains and 85% mass fraction of 45 kbp rings.

A 48.5 kbp ( $3.15 \times 10^7$  g/mol) lambda ( $\lambda$ ) phage DNA was chosen as the linear counterpart to the rings. At the same total concentration, lambda DNA has a near equal degree of entanglement,  $Z$ , as the linear form of the FOS45 DNA and the difference in their respective molecular weights can be neglected. Importantly, both the FOS45 and the  $\lambda$ -phage DNA are monodisperse. The dynamics of entangled lambda DNA at different concentrations have been reported previously by Banik et al.<sup>40</sup>

*Lambda DNA (48.5 kbp) and FOS45 DNA (45 kbp) Were Not Mixed in Any of the Samples to Get a Blend.* In this work, two different FOS45 ring–linear blends were studied based on the mass fraction of the rings and linear chains present: (1) 85% rings and 15% linear chains; (2) 50% rings and 50% linear chains. We refer to the

percentage of linear chains present in the blends as  $\phi_{Lin}$  and the total concentration of the samples as  $\phi_{Tot}$ . We report viscoelastic measurements of the blends at three different total concentrations:  $\phi_{Tot} \sim 0.8, 1,$  and  $2$  mg/mL. To understand the effect of linear chains and total concentration, we compare the dynamics by keeping one of them constant at a time and varying the other. This allows us to understand their effects on the dynamics separately. Studying the dynamics of the blends provides a better understanding of the interactions of the two topologies as well as of the specific effects of linear chain contamination on ring viscoelasticity. The dynamics of the FOS45 blends is compared with the dynamics of linear  $\lambda$  DNA (100% linear counterpart) at the same total concentrations,  $\phi_{Tot}$ . The exact concentrations and the ring–linear compositions in the samples are given in Table 1. The uncertainty in the concentration measurements is  $\pm 0.05$  mg/mL. Hence, for simplicity and clarity while comparing, the concentrations of the blends and linear DNA are approximated as 0.8, 1, and 2 mg/mL (given in the parentheses in Table 1) in the Discussion section. The uncertainty in the linear chain concentration is  $\pm 2\%$ .

The radius of gyration of FOS45 has been probed experimentally by single molecule techniques.<sup>41</sup> The radius of gyration for the linear chain is calculated as  $R_{g,L} = \sqrt{LL_p/3}$ . DNA has a persistence length of  $L_p \sim 50$  nm,<sup>42,43</sup> which is stiffer than a conventional synthetic C–C chain and is considered semiflexible. The contour length,  $L$ , is estimated to be  $16.5 \mu$ m ( $306 L_p$  for FOS45 DNA). Larson and co-workers<sup>44,45</sup> had shown previously that if the DNA chain is sufficiently long, it can be assumed to be freely jointed chain. For the fosmid blend, the  $R_g$  values for both the ring and the linearized form are given in Table 2.  $R_{g,C}$  is the observed radius of gyration of the ring, and  $R_{g,L}$  is the calculated radius of gyration of its corresponding linearized form. The overlap concentration is given by  $\phi^* = \left[ M / \left( \frac{4\pi}{3} R_g^3 N_A \right) \right]$ , where  $M$  is the molecular weight and  $N_A$  is Avogadro's number. The entanglement concentration of linear DNA is calculated as  $\phi_e = 9\phi^*$ .<sup>46</sup> The number of entanglement per chain for the linear chains is calculated as  $Z = (\phi_{Tot}/\phi_e)^{1.25}$ .<sup>47</sup>  $Z$  is calculated based on the overlap and entanglement concentration of the DNA. In our linear DNA paper,<sup>40</sup> we recognize that different groups had previously reported different equations for calculating the entanglement concentration from the overlap concentration. In ref 40 we used  $(\phi_e = 9\phi^*)$  following the works of Liu et al.<sup>46</sup> and Musti et al.<sup>48</sup> The equation underestimates the  $Z \sim 8$  (assuming 100% linear chains) for the highest concentration (2 mg/mL). On using  $\phi_e = 4\phi^*$  following the work of Zhou and Schroeder,<sup>49</sup> we would obtain  $Z \sim 23$ . From the Likhtman–McLeish<sup>50</sup> model

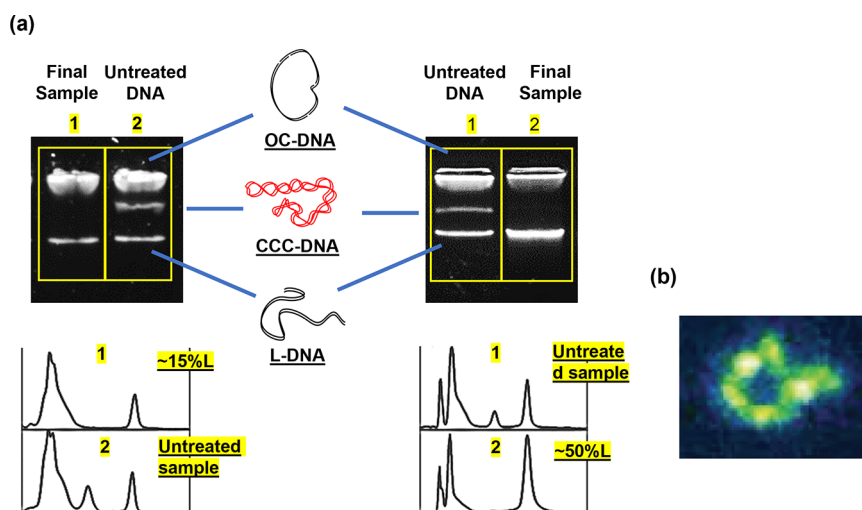


**Figure 3.** (a) Gel electrophoresis of fluoresced DNA samples showing all the three isoforms when untreated and the final samples with 15%L (lane 1 in left gel image) and 50%L (lane 2 in right gel image) as observed under a transilluminator. A 0.7% agarose gel was run at 60 V for 1–3 h. OC-DNA is the relaxed circular topology, CCC-DNA is the supercoiled topology, and L-DNA is the linear topology. The different lanes in the gel are marked. The intensity analysis confirming the different percentage of linear chains present (15 or 50%) in the final sample is given below the gel images. (b) A single molecule image of OC FOS45DNA ( $2.9 \times 10^7$  g/mol). The image is obtained by fluorescence imaging of a trapped DNA in a microfluidic device.<sup>53</sup>

predictions on the linear DNA LVE,  $Z \sim 61$  was predicted with the constraint release parameter  $c_v = 1$  and  $Z \sim 101$  with a constraint release parameter  $c_v = 10$  ( $c_v = 10$  provided a better fit to the LVE). The  $Z$  values for linear DNA obtained from different methods are given in Table 2. The entanglement densities along with the size, molecular weight, radii of gyration, and the overlap concentration of the two different DNA strains used in this work are also given in Table 2. The number of entanglements per chain for ring–linear blends would be different from that of the linear polymers at the same concentration  $\phi_{\text{Tot}}$ . Because there is no available method to calculate  $Z$  for the blends, we refer to the entanglement density of the blends corresponding to the 100% pure linear counterpart. Halverson et al.<sup>32</sup> and Parisi et al.<sup>24</sup> give good discussions regarding entanglement in ring–linear blends and provide viscosity behavior with linear chain percentage via molecular dynamics and experimental analysis, respectively.

It is also true that the concept of polymer entanglements in ring polymers can be interpreted from observation of topological interactions/constraints. Based on this concept, ring samples that do not show any plateau in their rheological behavior can still be considered as entangled. Although this concept is used in molecular simulations and in scattering experiments, it is difficult to verify experimentally for large molecular weight and concentrated systems. Readers must keep in mind how the system is deemed entangled or unentangled by different authors and not be confused by it. Here we use the metric that a system is entangled in the classical sense when it exhibits a rubbery plateau.

**2.2. Ring DNA, Cell Growth, Extraction, and Characterization.** Ring DNA was extracted from *E. coli* following a modified procedure put forward by Laib et al.<sup>41</sup> The extraction and the purification steps are described briefly in this section. Bacterial cells were grown overnight in LB (Luria–Bertani) broth. The time, volume, and aeration for the bacterial culture were optimized to ensure maximum growth of the cells while still in the exponential growth phase. The culture was then centrifuged at 5000 rpm for 8 min to collect the cells. The cells were resuspended in a Tris-EDTA (ethylenediaminetetraacetic acid)/TE buffer, followed by lysis in an alkaline buffer (NaOH, SDS = sodium dodecyl sulfate) which was then neutralized with a potassium acetate buffer (pH = 5.5). Following the lysis step, the medium becomes very viscous due to the release of cell debris, proteins, and the RNA and DNA (chromosomal and fosmid). Extreme care in handling was taken to avoid shear degradation of the circular fosmid DNA. The proteins and the chromosomal DNA were precipitated in the lysis–neutralization steps and removed following centrifugation at 10000 rpm for 45 min. The DNA in the supernatant was precipitated by

adding isopropanol and washed by using a 70% ethanol solution to remove the excess salts and isopropanol. Following the wash step, the DNA pellet was then dissolved in the TE buffer. The concentration of the DNA solution after all the treatments was usually around 0.02–0.1 mg/mL. To concentrate the samples, the dilute DNA was reprecipitated by using the ethanol and sodium acetate solution (1/10 vol, 3 M, pH = 5.2), and then the desired amount of TE buffer was added to redissolve the DNA pellets to obtain the desired concentration. NaCl is included in the TE-buffer recipe as EDTA-2Na to screen out the negative charge of the DNA.

In vivo, fosmid DNA are present in the supercoiled form, also called covalently closed circular (CCC) DNA. During the lysis of the cells, the supercoiled DNA is nicked (discontinuity in one of the two strands) at different positions along its length under the effects of chemical reagents, relaxing the torsional stress required to keep the supercoiled conformation thus forming open circular (OC) DNA. The OC DNA is of true circular topology and is used as our model ring polymer. Because the nicking is random, often a supercoiled DNA is nicked at the same position on both strands, converting the ring into the linearized conformation (L) DNA. Hence, linear chains are introduced in the system due to the chemical agents and/or mechanical shear. Generally, all three isoforms of DNA (CCC, OC, and L) are found after the extraction. To control either of these isoforms, we employ enzymes that can be used to convert one form to another or digest them. To linearize CCC-DNA and OC-DNA to L-DNA, an endonuclease enzyme (ApaI # R0114S, New England Biolabs) was used. To convert CCC-DNA to OC-DNA, a nicking enzyme (Nt.BstNBI, #R0607S, New England Biolabs) was used. To digest L-DNA, an exonuclease enzyme (RecBCD, #M0345S, New England Biolabs) was used. The different enzymes used in interconverting the topologies, the enzyme activities, and the titrated volumes required for digestion along with the purification steps are reported in detail in Laib et al.<sup>41</sup> and Robertson et al.<sup>51</sup> The restriction enzymes are highly active and selective and are cognizant of specific sites in the DNA. The minimum volumes of enzymes required to digest/convert per unit mass of DNA have been calculated before<sup>41</sup> which can be upscaled or downscaled based on the sample concentration and the molecular weight of the DNA. Gel electrophoresis and pulse field gel electrophoresis were used to characterize the DNA isoforms and to verify the sample purity. The percentage of OC/CCC/L DNA isoforms in a given fosmid sample is determined by gel electrophoresis (FisherBiotech FB-SB-710). Figure 3b shows samples with the different isoforms of DNA after extraction as visualized by gel electrophoresis along with samples with select isoforms following enzyme treatment. Different isoforms are found to traverse at

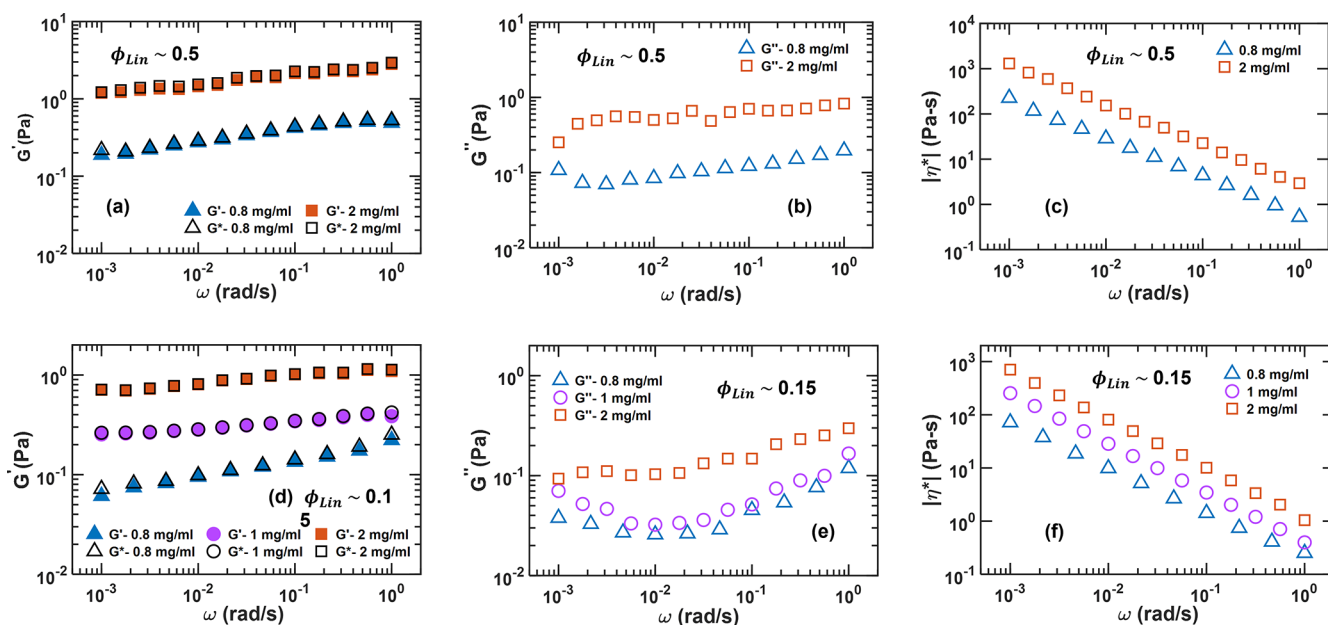


**Figure 4.** Frequency sweep results for ring–linear blend with  $\phi_{Lin} \sim 0.5$  at different total concentrations,  $\phi_{Tot} \sim 0.8$  and 2 mg/mL. (a) Storage and dynamic moduli vs angular frequency. (b) Loss moduli vs angular frequency. (c) Dynamic viscosity vs angular frequency. Frequency sweep results for ring–linear blend with  $\phi_{Lin} \sim 0.15$  at different total concentrations,  $\phi_{Tot} \sim 0.8, 1,$  and 2 mg/mL. (d) Storage and dynamic moduli vs angular frequency. (e) Loss moduli vs angular frequency. (f) Dynamic viscosity vs angular frequency.

different rates through the agarose gel, thus separating in different bands and characterized by selective enzymatic digestion. The relative proportion of the isoforms present in a sample can be estimated upon staining the DNA with a fluorescent dye (Gelstar, Lonza) and measuring the intensity of the fluoresced bands under a transilluminator (FE0350, FluorChem E). In the current work, we have made rigorous efforts to quantify the linear chains present in the sample (linear chains being considered as a contaminant) to thoroughly identify the composition of the DNA samples. Although ring DNA samples with 3–4% linear chain fraction could be obtained in small quantities (up to 20  $\mu\text{g}$  of DNA) following the enzyme digestion (exonuclease enzyme removes linear DNA), samples with  $\sim 15\%$  linear chain fraction could only be produced in bulk quantities due to the enzymes not reaching 100% conversion in large reaction volumes. Restriction enzymes are the most expensive reagents in the preparation. In the future work, the present endeavor will be carried forward, and the samples with  $<15\%$  linear chain contamination will be produced by using excess enzymes and possibly dividing the bulk samples into several hundred microassays.

The final concentrated samples were treated with RNase (New England Biolabs) to remove RNA and purified by using a phenol chloroform extraction method<sup>52</sup> to remove any proteins, enzymes, and the residual digested nucleic acids. The system was then membrane dialyzed (300 kDa MWCO, Spectra Por) against TE Buffer. The enzyme treatment and the purification steps reduce the DNA yield by 40–50%. Several of these were repeated until DNA samples of the required purity were obtained. The concentration of the DNA was also measured by a nanodrop spectrophotometer (Nanodrop 2000 C, Thermo Fisher Scientific). An absorbance ratio of  $\sim 1.9$  was found from the spectrophotometer measurement of the DNA, which is accepted as pure DNA. The measurements from both spectrophotometer and gel electrophoresis were matched to determine the concentration accurately.

For one of the samples (bulk rheology sample with  $\phi_{Lin} \sim 0.15$  and concentration  $\phi_{Tot} = 0.8$  mg/mL), there are some minor differences in some of the postextraction steps such as the use of spectra dehydrating gel to concentrate the DNA samples, and the final solution buffer was TE10 + 10 mM NaCl. Also, the exonuclease-V was not used in digesting the linear chains in those samples. The 10 mM NaCl is added so that the DNA can be treated as a neutral polymer. However, the dynamic results

and the scaling behaviors show that the additional charge in the buffer does not affect the observed rheological response at the reported entanglement densities and the dynamics is completely determined by the ring–linear entanglements.

### 2.3. Homogenization of the Concentrated DNA Solutions.

The homogenization of the concentrated samples is crucial. The concentrated DNA solutions obtained after the redissolving of the DNA pellet are not homogeneous. The concentration of the blobs is higher than the supernatant part of the DNA solution when measured by Nanodrop. In concentrated dispersions of DNA with very long relaxation times, the mechanical methods of homogenization may be ineffective, and the final solution may remain deceptively inhomogeneous. Our observation has been that the concentrated pockets in the solution cannot be pipetted (due to these blobs being almost gel like at high concentrations), nor can they be broken by mechanical agitation but rather unravel and diffuse over time and with higher temperature. In our previous work on linear  $\lambda$  DNA solutions<sup>54</sup> we had developed a systematic method to homogenize the concentrated DNA solutions. The homogenization protocol used in the present work was altered because the relaxation times of the ring–linear DNA blends are much longer than those of the 100% linear DNA at the same concentration, thus increasing the time required to completely mix and homogenize. The very long relaxation times can be observed in the dynamic data that are shown in a later section. In addition, we found that the open circular DNA is more prone to shear degradation or mechanical agitation into its linear isoform due to the nicks on its strands. Nicks are introduced in the nicking step which leads to single-stranded sites that are weaker than the double-stranded DNA itself. Hence, the commonly used mechanical mixing methods could not be applied to homogenize the ring–linear DNA blends, and we resorted to heating and very gentle pipetting with wide bore pipettes to accelerate the homogenization process. The samples were repeatedly incubated at room temperature and then heated to 45  $^{\circ}\text{C}$  for up to 5–7 weeks depending on the total concentration. Any residual inhomogeneous blobs were centrifuged, and the supernatant solution in the tube was taken as the sample for the rheological measurements. The concentration of the supernatant was measured by using the nanodrop instrument at three different positions in the top, middle, and the bottom parts of the tube. When the variation in the measurements was less than  $\pm 50$   $\mu\text{g}/\text{mL}$  (0.05 mg/mL), the solution was considered as homogeneous and used for the rheological

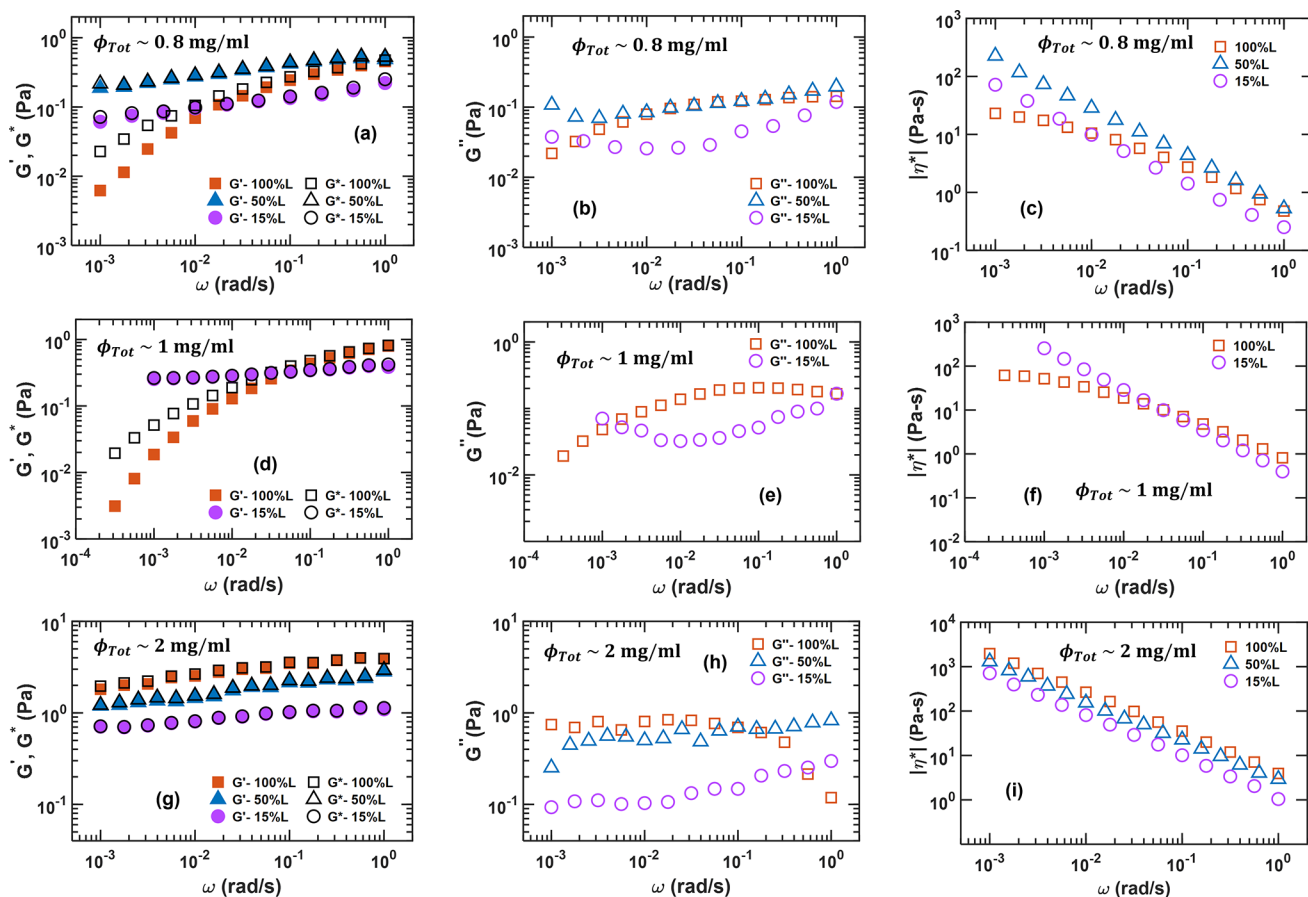


**Figure 5.** Frequency sweep comparison at different linear chain fractions. At a total concentration,  $\phi_{Tot} \sim 0.8$  mg/mL. The samples are compared at  $\phi_{Lin} \sim 0.15, 0.5$ , and  $1.0$ . (a) Storage and dynamic moduli vs angular frequency. (b) Loss moduli vs angular frequency. (c) Dynamic viscosity vs angular frequency. At a total concentration,  $\phi_{Tot} \sim 1$  mg/mL. The samples are compared at  $\phi_{Lin} \sim 0.15$  and  $1.0$ . (d) Storage and dynamic moduli vs angular frequency. (e) Loss moduli vs angular frequency. (f) Dynamic viscosity vs angular frequency. At a total concentration,  $\phi_{Tot} \sim 2$  mg/mL. The samples are compared at  $\phi_{Lin} \sim 0.15, 0.5$ , and  $1.0$ . (g) Storage and dynamic moduli vs angular frequency. (h) Loss moduli vs angular frequency. (i) Dynamic viscosity vs angular frequency.

measurements. The concentration measurements from the nanodrop spectrophotometer and gel electrophoresis were also matched. A gel electrophoresis was performed before and after the rheological measurements to ensure the amounts of rings and linear chains present in the sample had not changed significantly.

Rigorous measures were taken to ensure that the sample is homogeneous. To ensure homogeneity, the concentration was characterized via nanodrop measurement, and a narrow uncertainty of  $50 \mu\text{g/mL}$  was maintained in all the samples. We are certain of the linear chain impurity (within  $\pm 2\%$ ) in the blend sample. We have made thorough efforts to characterize the blend samples and no impurities other than ring and linear DNA in the composition could be detected by different characterization methods. The percentage of linear chains in a blend sample is also confirmed by single molecule counting by the Schroeder group with the help of single molecule visualization methods. In the single molecule counting protocol, the DNA molecules are hydrodynamically trapped one at a time and the topology of the molecule is ascertained by chain stretching.<sup>55</sup> This method is repeated for 100 DNA molecules, and the composition of rings and linear chains out of 100 molecules is estimated.

**2.4. Rheological Measurements.** Two different rheometers (AR G2 and Hybrid 2, TA Instruments) were used to conduct the tests. The 25 mm stainless steel parallel plate geometries were used for the rheological measurements. A Krytox oil solvent trap (Krytox 100) was utilized to minimize the evaporation of water. All the measurements were done at  $25^\circ\text{C}$ . The aqueous buffer can be considered to be a good solvent at this temperature. Samples were loaded all at once on the plates by using a micropipet to avoid formation of bubbles. The gap

between the plates were fixed between 350 and 500  $\mu\text{m}$  depending on sample volume available and concentration. The samples were collected after running the tests, and the total DNA concentration and linear percentage were measured by nanodrop and gel electrophoresis. The concentration and linear percentage of the ring–linear blends were found to be the same both before and after the rheological testing within the experimental uncertainties.

Stress sweep tests were conducted at 1, 0.1, 0.01, and 0.001 rad/s prior to frequency sweeps to determine the linear response regime. Frequency sweeps were conducted after fixing the stress inside the linear regime. The angular frequencies were swept from 1 to 0.001 rad/s, and 4–5 data points were taken per decade.

### 3. RESULTS AND DISCUSSION

**3.1. Oscillatory Frequency Sweeps on Ring–Linear DNA Blends.** **3.1.1. Effect of Total Concentration,  $\phi_{Tot}$ .** In this section, the frequency sweep results of the blends are compared at different total concentration  $\phi_{Tot}$  keeping the linear chain fraction  $\phi_{Lin}$  constant. The results from the dynamic tests are given in Figure 4. In Figures 4a–c, the data at a constant linear chain fraction of  $\phi_{Lin} \sim 0.5$  are presented at total concentration  $\phi_{Tot}$  of  $\sim 0.8$  and 2 mg/mL. In Figures 4d–f the data at a constant linear chain fraction of  $\phi_{Lin} \sim 0.15$  are presented at different total concentrations  $\phi_{Tot}$  of  $\sim 0.8, 1$ , and 2 mg/mL. From the storage and the loss moduli results (Figures 4a,b and 4d,e), it is evident that the blends at both the linear chain

fractions  $\phi_{\text{Lin}} \sim 0.15$  and  $0.5$  are in the rubbery regime in the test window. The  $G'$  is entirely flat resembling the rubbery plateau region. The dynamic modulus,  $G^*$  (black symbols), is also plotted in Figure 4a,d and matches almost identically with the  $G'$  magnitude, thus confirming the data to be in the rubbery regime. The loss modulus,  $G''$ , data are noisy due to the softness of the solutions and the response being at the low limit of instrument torque sensitivity. A higher total concentration produced a greater magnitude of the plateau modulus,  $G_N^0$ . The dynamic viscosity,  $|\eta^*|$ , in Figure 4c,f shows a power law trend over the entire range of angular frequencies. With increase in concentration, the dynamic viscosity increases monotonically. Upon comparison of Figures 4c and 4f, it can be surmised that in the DNA blends with a decrease in %L from 50 to 15%, the frequency dependence (slopes) of the dynamic viscosity is the same independent of the linear concentration; only the magnitudes are different.

**3.1.2. Effect of Linear Chain Concentration,  $\phi_{\text{Lin}}$ , on Ring–Linear Blends and Comparison with 100% Linear DNA.** In this section, the frequency sweep results are compared at a constant total concentration,  $\phi_{\text{Tot}}$  at different linear chain concentrations,  $\phi_{\text{Lin}}$ . Figures 5a–c, 5d–f, and 5g–i show the dynamic results at a constant total concentration,  $\phi_{\text{Tot}} \sim 0.8, 1,$  and  $2$  mg/mL, respectively, at different linear chain fractions and compare them with the response for the 100% linear DNA.

From Figure 5a, we see that  $G'$  of the 100% linear DNA shows a transition from the rubbery regime to the terminal regime with decrease in  $\omega$ . Different from the 100% linear solutions, the ring–linear DNA blends (even with only 15% linear chains) are entirely in the rubbery regime and do not show any transition even at a low  $\phi_{\text{Tot}} \sim 0.8$  mg/mL. The difference in the behavior can also be ascertained by observing the dynamic moduli (black symbols) in Figure 5a. Particularly interesting is the blend with 15% linear fraction, whose plateau modulus ( $G_N^0$ ) at the highest frequency is lower than the 100% linear chain, but the storage modulus,  $G'$ , does not change as drastically with decrease in angular frequency. This difference in behavior is also observed in the dynamic viscosity as seen in Figure 5c. The dynamic viscosity  $|\eta^*|$  for the 100% linear DNA reaches the Newtonian viscosity  $\eta_0$  at  $\sim 0.001$  rad/s, but for the 15%L and 50%L solutions  $|\eta^*|$  continues to follow a power law-like increase; viz., the Newtonian plateau is not reached at low frequency in either of the blends. Thus, the  $\eta_0$  of ring DNA blends with 15%L and 50%L would be much higher than that of the analogous linear DNA solution at the same concentration. In fact, a closer look at Figure 5c shows that the dynamic viscosity of the 15%L and the 50%L blend is greater than that of the 100%L sample by at least a factor of 3 and 10, respectively. This is a much greater effect than reported by any other studies on synthetic “contaminated” rings even if the dynamic viscosities measured in the current system have not reached the Newtonian plateau. This behavior is quite different from that of the synthetic melts as shown in Figure 2 where the blend viscosity is higher at most by a factor of 2–3 times that of the 100% linear analogue’s viscosity.

Figures 5d–f shows the comparisons between the 15% linear blend and 100% linear DNA at the total concentration of  $\phi_{\text{Tot}} \sim 1$  mg/mL. The same trend as in Figures 5a–c is observed here as well. In the storage modulus, the final magnitude of the plateau modulus of the blend is lower than that of the 100% linear DNA, but the blend LVE remains nearly constant at all  $\omega$ . The broadening of the plateau in the 15% blend is discernible from the dynamic modulus,  $G^*$ , data. The 100% linear DNA solution is at the steady state viscosity  $\eta_0$  at  $0.001$  rad/s, while the  $|\eta^*|$  for

the 15%L blend is still increasing. The final  $\eta_0$  of the 15%L blend at  $1$  mg/mL would be much greater than a factor of 6 than that of 100% linear DNA solution.

From Figure 2, in the synthetic melts the 100% linear PS had a greater viscosity than the mixtures with 0–30% linear chain percentage. From our current results, the sample with only 15% linear chains shows a much greater viscosity than its pure linear counterpart. It suggests that the impact of linear chain contaminants on the dynamics of the pure rings was lower in the case of synthetic polymer melts. Further work is required to establish the exact relationships.

Figures 5g–i show comparisons of dynamic responses of the ring/linear blends with the responses of the 100% linear DNA at a total concentration of  $\phi_{\text{Tot}} \sim 2$  mg/mL. All three samples are entirely in the rubbery regime, and we do not see a transition to the terminal regime in either storage modulus or the dynamic viscosity. The magnitude of  $G'$  for the 100% linear DNA is greater than that of the blends and shows a greater final plateau modulus,  $G_N^0$ . At  $2$  mg/mL, the dynamic viscosity of the 100% linear DNA is greater than that of the blends in the entire range of angular frequency tested. This is interesting and was not observed at  $0.8$  and  $1$  mg/mL. Clearly, the entanglement effect of the 100% linear DNA at this concentration exceeds the blends. The dynamic data here at the different concentrations show that the impact of linear chains on ring dynamics is sensitive not only to the entanglement density and the amount of linear chains but also on the total polymer concentration in the solution.

The 100% linear DNA show long relaxation times as reported by Banik et al.<sup>40</sup> In comparison to that the ring–linear blends showed an even longer relaxation time. Even the blend with only 15% linear chain fraction at the lowest concentration of  $0.8$  mg/mL showed no signs of transitioning to the terminal Newtonian flow regime from the entangled rubbery regime after three decades of angular frequencies tested. The increase in projected zero shear viscosity in the blends over that of the linear counterpart is multiple factors greater than previously reported for polymer melts for any linear/ring composition. However, the relative plateau modulus magnitudes are similar to those observed in synthetic melt ring/linear blends. This is further described later in the discussion of the normalized plateau moduli of the blends following the approach proposed by Roovers in his work for PS ring–linear blends (Figure 8).<sup>26</sup> Also, on visual inspection of the LVE in the reported synthetic melts, the rubbery plateau region (or the development of the plateau) has been shown to appear gradually and monotonically from power law relaxation to entangled with increase in linear chain content.<sup>13,22</sup> However, an increase in the rubbery region in ring–linear mixtures by at least an order of magnitude relative to its linear counterpart has not been reported in the literature to the best of our knowledge. In fact, the creep experiments from McKenna et al.<sup>8</sup> seemed to show the rubbery plateau of the rings (now thought to be contaminated by linear chains) exhibited a shorter rubbery plateau regime than did the linear counterparts, and similar inferences can be made from the data reported by Roovers<sup>28</sup> in his studies of polybutadiene rings mixed with linear chains. The more recent studies of ring dynamics<sup>13,14,21</sup> suggest no rubbery plateau for ring melts having up to  $\sim 15$  entanglements. Kapnistos et al.<sup>13</sup> showed a small increase in the relaxation time on adding linear chains (at  $\sim 20\%$  linear fraction) but only in the terminal region. Parisi et al.<sup>24</sup> also reported an increase in the terminal relaxation time in the PS ring–linear blends with 30% ring fractions but only by a much

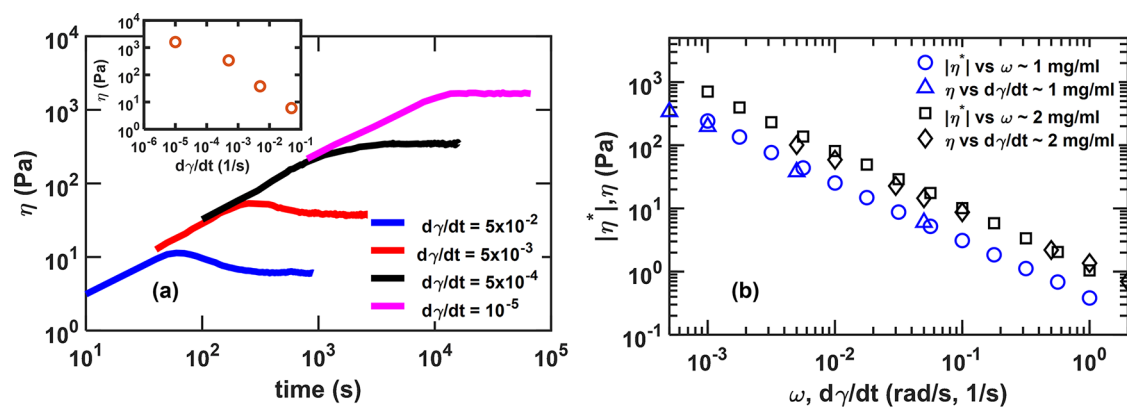


**Figure 6.** (a) Steady shear results on ring–linear blend with  $\phi_{\text{Lin}} = 0.15$  at a concentration  $\phi_{\text{Tot}} \sim 1$  mg/mL. The inset shows the plot of viscosity vs shear rate. (b) Cox–Merz equivalence for ring–linear blend with  $\phi_{\text{Lin}} = 0.15$  at concentrations  $\phi_{\text{Tot}} \sim 1$  and 2 mg/mL.

smaller factor of 2, and their entanglement plateau also did not show any noticeable increase in its breadth. Clearly, for DNA ring–linear blends the terminal relaxation times will probably scale very strongly with linear chain percentage because the plateau modulus itself has a weaker linear chain concentration dependence. Such increase in relaxation time in the blends can be attributed to threading of the rings by linear chains.<sup>56–58</sup> The threading effects determining the increase in viscosity are a function of the correlation length which is determined by both polymer concentration and molecular weight. Because the polymer concentrations in the DNA solutions are very low ( $\phi_{\text{Tot}} \sim 1$  mg/mL is  $\sim 0.1$  wt %), the molecular weight is playing a significant role in determining the correlation length. Clearly, the effect of linear contaminants in these solutions is much greater than what is observed in the melts. Why the effect is so much stronger in the current solution studies compared to the melt studies requires future investigation. It could be argued that solution behavior is distinctly different from melts and the consequent scaling might be greater than in melts. But entanglement in ring solution is not known to be distinct, and we have no evidence of that conclusion yet. Moreover, polymer solutions have been considered to rheologically similar to polymer melts,<sup>59,60</sup> and whether the two systems show different behavior or not can only be ascertained by comparison (Roovers plots). The stiffness of DNA can also contribute to the increase in relaxation time. DNA has a persistence length of  $\sim 50$  nm,<sup>42,43</sup> which is much stiffer than a conventional synthetic C–C chain and is considered semiflexible. However, Larson and co-workers<sup>44,45</sup> had shown previously that if the DNA chain is sufficiently long, it can be assumed to be freely jointed chain. It can be argued that at high concentrations the solution correlation length and the distance between neighboring strands of ds-DNA decrease to length scales smaller than the Kuhn length, and the DNA might behave as semiflexible or even rigid-like at such length scales. However, highly entangled calf thymus DNA has been shown to exhibit scaling like synthetic polymers.<sup>61,62</sup> In our linear DNA paper, Banik et al.<sup>40</sup> also observed that the concentration scaling is like concentrated synthetic polymer solutions from Heo and Larson.<sup>60</sup> Also, there is no evidence yet whether chain stiffness would increase or decrease threading of rings by the linear chains or to what extent.

In blends, estimating the entanglement density is complicated as four different types of entanglement dictate the dynamics: ring in linear, linear in ring, linear in linear, and ring in ring. The presence of the rings and linear chains and the interspecies threading lead to very high zero-shear rate viscosity  $\eta_0$  in the

blends compared to the linear–linear entanglements in the 100% linear solution. Robertson et al.<sup>63</sup> showed that self-diffusion coefficient of circular DNA surrounded by linear DNA is the smallest among the four possible cases at  $C > C^*$ . Whether it is still the determining step in relaxation of molecules in well-entangled systems is not known. Rings have also been suggested to form topological glass from modeling endeavors.<sup>64,65</sup> To study whether blends of rings and linear chains also form topological glass or not would be interesting as a future work.

Despite the low plateau modulus values, the zero-shear viscosity of the blends could not be achieved in the frequency range tested. To extract the zero shear rate viscosities, tests must be performed at lower angular frequencies, or a time–concentration superposition type method would have to be applied. This led us to perform steady shear experiments. In the next section, we show a test result that even at shear rates as low as  $10^{-5} \text{ s}^{-1}$  the blends did not reach the Newtonian flow regime.

**3.2. Increase in Relaxation Time and the Cox–Merz Rule.** The zero-shear viscosity was not observed in the dynamic data as the results showed the blends to be in the rubbery regime over the 3 decades of angular frequency tested down to  $10^{-3}$  rad/s. Although steady shear tests on the blends were conducted, we do not present the full results from the nonlinear rheology in this article. The nonlinear shear startup results for a single sample are presented here to conform and somewhat extend the dynamic oscillation results and to emphasize the large increase in the steady shear viscosity that is observed in the blends. Figure 6a shows that the shear startup and the zero-shear viscosity. For the blend with  $\phi_{\text{Lin}} = 0.15$ , a  $\phi_{\text{Tot}} \sim 1$  mg/mL the zero shear rate viscosity is not reached even at a shear rate of  $10^{-5} \text{ s}^{-1}$ . In comparison, at 1 mg/mL the zero-shear viscosity for the 100% linear lambda DNA is reached at  $\sim 5 \times 10^{-4} \text{ s}^{-1}$ , thus showing an increase in time to reach the zero-shear viscosity by at least a factor of 50. It must be noted that though we see an  $\sim 50$  times increase in viscosity in the blends, the plateau modulus,  $G_N^0$ , for the blend is smaller than that for the 100%L sample by a factor of  $\sim 3$ . We anticipate that the increase in time to reach the zero-shear viscosity would be even greater for higher linear chain fraction,  $\phi_{\text{Lin}} = 0.5$ , and at higher total concentration,  $\phi_{\text{Tot}}$ .

Following the steady shear tests, we compared the shear and dynamic test results. In Figure 6b, the Cox–Merz rule is seen to hold for the 15% linear chain blend at both 1 and 2 mg/mL concentration. The Cox–Merz rule is an empirical equivalence of the nonlinear steady shear viscosity and the linear dynamic viscosity.<sup>66</sup> The dynamic viscosity dependence on angular frequency was obtained from the frequency sweep tests, and the

shear viscosity dependence on shear rate was obtained from the steady shear tests. The steady shear measurements were corrected for the nonuniform strain in the parallel plate geometry with the Rabinowitsch-type correction.<sup>67</sup> No discernible changes in the data were found following the correction. From the inset in plot Figure 6a, a shear thinning exponent of  $0.75 \pm 0.09$  can be estimated for the ring-linear DNA blend with 15%L at 1 mg/mL. Yan et al.<sup>68</sup> reported a close 0.79 shear thinning exponent for PS ring-linear blends with 85% linear fraction. The authors showed that the shear thinning exponent reduces with decrease in linear chain fraction. In their paper, they found the exponent to reduce from 0.85 for 100% linear chains to 0.44 for nearly pure ring samples (possibly 1–10% linear content), suggesting weaker nonlinear deformation in the rings. Parisi et al.<sup>38</sup> gave a systematic comparison of the shear thinning exponents and showed an exponent of  $\sim 0.89$  for 100% linear, exponent of 0.85–0.89 for blends, and an exponent of 0.56 for rings from model and molecular dynamics predictions. In this work, the shear thinning exponent for the blend with 15% L is only moderately less than the shear thinning exponent,  $\sim 0.88$  for 100% linear DNA (not shown here). The small change in the exponent shows that the presence of 15% linear chain affects the dynamics almost the same if the system were 100% linear chains. This is also discernible from the plateau modulus scaling, discussed in the next section.

**3.3. Dependence of Rubbery Plateau Modulus  $G_N^0$  on Total Concentration  $\phi_{\text{Tot}}$  and Linear Chain Fraction  $\phi_{\text{Lin}}$ .** The rubbery plateau modulus  $G_N^0$  is an important parameter to describe the entanglements in a polymer. By convention,  $G_N^0$  is selected from the storage modulus  $G'$  at the angular frequency where  $G''$  goes through a minimum. The  $G_N^0$  is chosen as such for the 15%L ( $\phi_{\text{Lin}} \sim 0.15$ ) samples where the minimum in the  $G''$  is observed. The minimum is not observed for the 50% ( $\phi_{\text{Lin}} \sim 0.5$ ) samples. We assume the storage modulus at the highest measured  $\omega = 1$  rad/s as the plateau moduli. A standard error for each of the fit is provided since the true plateau moduli could not be observed for the some of the blends. The  $G_N^0$  for the linear lambda DNA at different concentrations have been reported in Banik et al.<sup>54</sup> The  $G_N^0$  for the blends and linear solutions are listed in Table 3.

**Table 3.  $G_N^0$  and  $G_{N,\text{blend}}^0/G_{N,L}^0$  for the Ring-Linear DNA Blends and 100% Linear DNA**

| L% ( $\phi_{\text{Lin}}$ ) | $\phi_{\text{Tot}}$ (mg/mL) | $G_N^0$ (Pa) | $G_{N,\text{blend}}^0/G_{N,L}^0$ |
|----------------------------|-----------------------------|--------------|----------------------------------|
| 15                         | 0.8                         | 0.13         | 0.26                             |
|                            | 1                           | 0.2          | 0.25                             |
|                            | 2                           | 0.88         | 0.226                            |
| 50                         | 0.8                         | 0.3          | 0.6                              |
|                            | 2                           | 2.25         | 0.577                            |
| 100                        | 0.8                         | 0.5          | 1                                |
|                            | 1                           | 0.8          | 1                                |
|                            | 2                           | 3.9          | 1                                |

Figure 7a shows the plateau moduli for the DNA samples (blends and 100% linear) plotted as a function of total concentration. For  $\phi_{\text{Lin}} \sim 0.15$ , the  $G_N^0$  scaling is  $2.2 \pm 0.12$ , and  $G_N^0 \sim \phi_{\text{Tot}}^{2.2}$ . For  $\phi_{\text{Lin}} \sim 0.5$ , the  $G_N^0$  is  $2.25 \pm 0.16$ , and  $G_N^0 \sim \phi_{\text{Tot}}^{2.25}$ . For 100% linear chains, the  $G_N^0$  scaling is  $2.29 \pm 0.08$ , and  $G_N^0 \sim \phi_{\text{Tot}}^{2.29}$ . Because of the limited data only an approximate power law exponent can be obtained, and we suggest that  $G_N^0$  scaling exponent could be between 2 and 2.3. The scaling exponents for the blends at both  $\phi_{\text{Lin}}$  are close to

that of the 100% linear DNA within the experimental errors. It suggests that either at the lowest linear concentration tested here,  $\phi_{\text{Lin}} \sim 0.15$ , the linear chains are determining the plateau modulus scaling or if rings had a plateau modulus it might scale in a similar fashion as do the linear chains.

The effect of linear chain content on the plateau modulus  $G_N^0$  is shown in Figure 7b. A power law behavior of  $0.78 \pm 0.08$  is observed at  $\phi_{\text{Tot}} = 2$  mg/mL,  $0.73 \pm 0.17$  at  $\phi_{\text{Tot}} = 1$  mg/mL, and  $0.75 \pm 0.1$  at  $\phi_{\text{Tot}} = 0.8$  mg/mL. Combining the two, we have  $G_N^0 \sim (\phi_{\text{Tot}})^{2.2-2.29}(\phi_{\text{Lin}})^{0.7-0.8}$  for the DNA blends tested in this work.

**3.4. Reduced  $G_N^0$  for the Ring-Linear Blends.** To compare the  $G_N^0$  for ring-linear blends of different materials, a reduced  $G_N^0$  parameter was employed by Roovers,<sup>8,26–28</sup> who investigated the ring and ring-linear blends of polystyrene (PS) and polybutadiene (PBD) melts. The reduced  $G_N^0$  provides a way to normalize the  $G_N^0$  measured for the ring-linear blends at different total concentrations and molecular weight. It is obtained by dividing the  $G_N^0$  of the ring-linear blend by the  $G_N^0$  of the 100% linear sample at the same concentration. The reduced  $G_N^0$  of the DNA blends are listed in Table 3. Figure 8 depicts a comparison of reduced  $G_N^0$  vs  $\phi_{\text{Lin}}$  for the DNA blends for the PS and PBD blends. The reduced  $G_N^0$  vs linear chain fraction for the PS and PBD blends was fitted to a curve to act as a guide to the eye. By plotting the synthetic ring melts and biological ring DNA solutions together, we intend to show that a Roovers plot-like scaling is obeyed by two very different types of ring polymers. As observed, the reduced  $G_N^0$  for the DNA blends falls closely on this fitting curve agreeing with the results reported by Roovers for polymer melts and that this kind of trend in reduced plateau modulus seems to be followed, at least approximately for both synthetic and biological ring/linear blends as well as in the melt and the entangled solution conditions. In Figure 8, the reduced  $G_N^0$  decreases with increase in total concentration at both the blend fractions. Though this trend cannot be confirmed just yet due to limited data and the uncertainties in the plateau moduli estimation, it would be interesting to find if it holds valid at other linear chain fractions as well. Although one might have anticipated that the normalized plateau modulus would be independent of the total DNA concentration, this does not seem to be the case. At 0.8 and 1 mg/mL the dynamics of the blends seemed more entangled than its linear counterpart (greater final plateau and viscosity). At 2 mg/mL the dynamics of the linear chain seemed more entangled. If we consider that there is a large increase in viscosity relative to the linear chains in the blends, this combined with the reduction in plateau modulus and its dependence on total concentration suggests that the way that the linear chains entangle with the rings is different from how they entangle with themselves. Perhaps this is not surprising as the network aspect related to the rubbery plateau and the dethreading required for viscous flow are different aspects of the entangled behavior. It is worth remarking that there is a possibility that the rings from the Roovers's studies<sup>19</sup> had more linear chain contamination in them than initially thought which would bring the data from this study and those from the reported studies closer together.

The Roovers plot can also be applied for reduced viscosity vs linear fraction. The figure is not shown here as the zero-shear viscosities for the DNA blends could not be estimated. The reduced viscosity for the DNA blends would not lie close to the melt PS data as the viscosity increase observed here is much greater than in the melts.

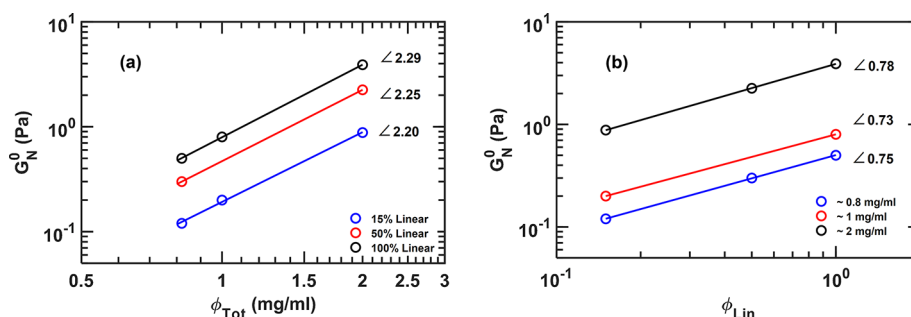


**Figure 7.** (a) Plot of  $G_N^0$  as a function of total concentration  $\phi_{Tot}$  for the blends with 15%L, 50%L, and 100% linear DNA. The lines are the fits to the data. (b) Plot of  $G_N^0$  as a function of linear chain fraction for the blends at 0.8, 1, and 2 mg/mL. The lines are the fits to the data.

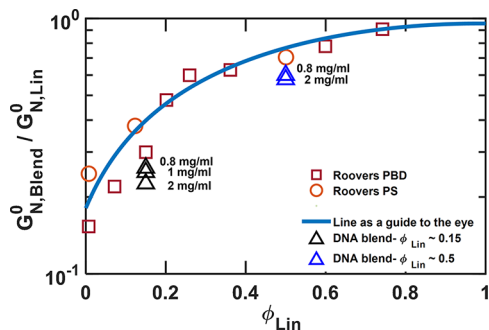


**Figure 8.** Reduced  $G_N^0$  vs linear chain ratio of the DNA blends and the ring–linear melts of polystyrene (PS) and polybutadiene (PBD) from Roovers' work.

Parisi et al.<sup>24</sup> predicted an increase of relaxation time of ring–linear blend with low composition of rings (<30% rings) with respect to linear melts by a factor of  $(M_{w,ring}/M_e)^2$ . In the future, we would like to test this by adding a small amount of DNA rings to linear DNA. It is of interest to traverse the entire nonmonotonic behavior by testing different compositions of the blends. This will also allow us to quantify the maximum in the scaled viscosity or the scaled plateau modulus plots (Roovers plots).

#### 4. CONCLUSIONS

In this work, monodisperse entangled ring/linear DNA blends (fosmid 45 kbp,  $2.9 \times 10^7$  g/mol) have been used to investigate the contribution of linear chains to ring dynamics as a function of total concentration  $\phi_{Tot}$  and relative amounts of linear and ring DNA  $\phi_{Lin}$ . The dynamics of the DNA blends is then compared to those of lambda-phage DNA (48.5 kbp,  $3.15 \times 10^7$  g/mol) as its 100% linear polymer analogue. This is the first effort to report the bulk rheology of circular (ring–linear blends) DNA and is the largest ring polymer studied so far in bulk to investigate the entanglement properties of the rings. Rigorous efforts were made to characterize and homogenize the concentrated DNA samples. The DNA blends in this work are probably the only ring samples until date which we can authenticate to have pure circular topology (devoid of knots or other nonlinear and noncircular structures) as they were visualized by single molecule imaging.

The presence of linear chains in the ring solutions alters the blends' properties significantly. First, the blends show an extended rubbery region compared to the pure linear counterpart but with a lower final plateau modulus,  $G_N^0$ . This trend is observed at both  $\phi_{Lin} \sim 0.15$  and 0.5. The dynamics stayed in the rubbery region over the 3 decades of angular frequencies tested.

The extension of the rubbery region has not been observed in the synthetic ring–linear melts reported in the literature. In the reported data the rubbery region has always been found to be shorter or comparable to that of the pure linear polymer.<sup>13,14,22</sup>

We attribute the extent of broadening of the dynamics to the ring–linear threading effects amplified by the very large molecular weight of the DNA molecules. The power law dependence for the plateau modulus  $G_N^0 \sim (\phi_{Tot})^{2.2-2.3}$  and  $G_N^0 \sim (\phi_{Lin})^{0.7-0.8}$  are obtained for the blends. It is important to note that the plateau modulus  $G_N^0$  of the blends is lower than that of the 100% linear system, but it is not diminished nearly as much as viscosity is increased. This provides evidence that the ring–linear threading only increases the relaxation time distribution and the viscosity scaling. The presence of the ring–linear threading leads to very high zero-shear rate viscosity  $\eta_0$  in the blends compared to the linear–linear entanglements in the 100% linear solution. The  $\eta_0$  for  $\phi_{Lin} = 0.15$  at  $\phi_{Tot} \sim 1$  mg/mL could not be observed even at a shear rate of  $\dot{\gamma} = 10^{-5} \text{ s}^{-1}$ . The Cox–Merz equivalence was found to hold for the blend solutions with 15% linear chain.

Considering the extremely long relaxation times and high  $\eta_0$ , it is a great challenge to investigate the rheological properties for the linear–ring blends at the concentrations used in this work. In future work, ring–linear blends at lower total concentrations and possibly with lower molecular weight DNA strains would be tested to explore the entire entanglement dynamics with total concentration and linear chain percentage. Dynamic tests on blends having a much lower linear chain concentration (1–5% L) to extrapolate the  $\phi_{Lin}$  to zero will be conducted. Tests will also be conducted on blends with low ring fractions and will be compared with the existing literature.

#### AUTHOR INFORMATION

##### Corresponding Author

Gregory B. McKenna – Department of Chemical Engineering, Texas Tech University, Lubbock, Texas 79409, United States; Department of Chemical and Biomolecular Engineering, North Carolina State University, Raleigh, North Carolina 27695, United States; [orcid.org/0000-0002-5676-9930](https://orcid.org/0000-0002-5676-9930); Email: [gbmckenn@ncsu.edu](mailto:gbmckenn@ncsu.edu)

##### Authors

Dejie Kong – Department of Chemical Engineering, Texas Tech University, Lubbock, Texas 79409, United States  
Sourya Banik – Department of Chemical Engineering, Texas Tech University, Lubbock, Texas 79409, United States  
Michael J. San Francisco – Department of Biological Sciences, Texas Tech University, Lubbock, Texas 79409, United States

Megan Lee — Department of Physics and Biophysics, University of San Diego, San Diego, California 92110, United States

Rae M. Robertson Anderson — Department of Physics and Biophysics, University of San Diego, San Diego, California 92110, United States; [orcid.org/0000-0003-4475-4667](https://orcid.org/0000-0003-4475-4667)

Charles M. Schroeder — Department of Materials Science and Engineering and the Department of Chemical & Biomolecular Engineering, University of Illinois at Urbana–Champaign, Urbana, Illinois 61801, United States; [orcid.org/0000-0001-6023-2274](https://orcid.org/0000-0001-6023-2274)

Complete contact information is available at:  
<https://pubs.acs.org/10.1021/acs.macromol.1c01672>

### Author Contributions

D.K. and S.B. contributed equally to this work.

### Notes

The authors declare no competing financial interest.

### ACKNOWLEDGMENTS

The authors acknowledge the following funding organizations for their support of this work. Texas Tech University: National Science Foundation under Grant CBET 1603943 and the J.R. Bradford endowment at Texas Tech University, each for partial support of this project. University of San Diego: Air Force Office of Scientific Research (Grant AFOSR-FA9550-17-1-0249) and the National Science Foundation (Grant NSF-CBET-1603925). University of Illinois Urbana–Champaign: National Science Foundation (NSF-CBET-1604038).

### REFERENCES

- (1) Richter, D.; Gooßen, S.; Wischnewski, A. Celebrating Soft Matter's 10th Anniversary: Topology matters: structure and dynamics of ring polymers. *Soft Matter* **2015**, *11* (44), 8535–8549.
- (2) McLeish, T. Polymers Without Beginning or End. *Science* **2002**, *297* (5589), 2005.
- (3) Semlyen, J. A. Cyclic polymers. *Pure Appl. Chem.* **1981**, *53* (9), 1797–1804.
- (4) Higgins, J. S.; Dodgson, K.; Semlyen, J. A. Studies of cyclic and linear poly(dimethyl siloxanes): 3. Neutron scattering measurements of the dimensions of ring and chain polymers. *Polymer* **1979**, *20* (5), 553–558.
- (5) Hild, G.; Kohler, A.; Rempp, P. Synthesis of ring-shaped macromolecules. *Eur. Polym. J.* **1980**, *16* (6), 525–527.
- (6) Hild, G.; Strazielle, C.; Rempp, P. Cyclic macromolecules. Synthesis and characterization of ring-shaped polystyrenes. *Eur. Polym. J.* **1983**, *19* (8), 721–727.
- (7) Geiser, D.; Höcker, H. Synthesis and Investigation of Macroscopic Polystyrene. *Macromolecules* **1980**, *13* (3), 653–656.
- (8) Roovers, J.; Toporowski, P. M. Synthesis and characterization of ring polybutadienes. *J. Polym. Sci., Part B: Polym. Phys.* **1988**, *26* (6), 1251–1259.
- (9) Roovers, J.; Toporowski, P. M. Synthesis of high molecular weight ring polystyrenes. *Macromolecules* **1983**, *16* (6), 843–849.
- (10) Bielawski, C. W.; Benitez, D.; Grubbs, R. H. An Endless Route to Cyclic Polymers. *Science* **2002**, *297* (5589), 2041.
- (11) McKenna, G. B.; Hostetter, B. J.; Hadjichristidis, N.; Fetters, L. J.; Plazek, D. J. A study of the linear viscoelastic properties of cyclic polystyrenes using creep and recovery measurements. *Macromolecules* **1989**, *22* (4), 1834–1852.
- (12) McKenna, G. B.; Plazek, D. J. The viscosity of blends of linear and cyclic molecules of similar molecular mass. *Polym. Commun. (Guildford)* **1986**, *27* (10), 304–306.
- (13) Kapnistos, M.; Lang, M.; Vlassopoulos, D.; Pyckhout-Hintzen, W.; Richter, D.; Cho, D.; Chang, T.; Rubinstein, M. Unexpected power-law stress relaxation of entangled ring polymers. *Nat. Mater.* **2008**, *7* (12), 997–1002.
- (14) Doi, Y.; Matsubara, K.; Ohta, Y.; Nakano, T.; Kawaguchi, D.; Takahashi, Y.; Takano, A.; Matsushita, Y. Melt Rheology of Ring Polystyrenes with Ultrahigh Purity. *Macromolecules* **2015**, *48* (9), 3140–3147.
- (15) Jeong, Y.; Jin, Y.; Chang, T.; Uhlik, F.; Roovers, J. Intrinsic Viscosity of Cyclic Polystyrene. *Macromolecules* **2017**, *50* (19), 7770–7776.
- (16) Bielawski, C. W.; Benitez, D.; Grubbs, R. H. Synthesis of Cyclic Polybutadiene via Ring-Opening Metathesis Polymerization: The Importance of Removing Trace Linear Contaminants. *J. Am. Chem. Soc.* **2003**, *125* (28), 8424–8425.
- (17) Molnar, K.; Helfer, C. A.; Kaszas, G.; Krisch, E.; Chen, D.; McKenna, G. B.; Kornfield, J. A.; Puskas, J. E. Liquid chromatography at critical conditions (LCCC): Capabilities and limitations for polymer analysis. *J. Mol. Liq.* **2021**, *322*, 114956.
- (18) Puskas, J. E.; Sen, S. Synthesis of Biodegradable Polyisobutylene Disulfides by Living Reversible Recombination Radical Polymerization (R3P): Macrocycles? *Macromolecules* **2017**, *50* (7), 2615–2624.
- (19) Lee, H. C.; Lee, H.; Lee, W.; Chang, T.; Roovers, J. Fractionation of Cyclic Polystyrene from Linear Precursor by HPLC at the Chromatographic Critical Condition. *Macromolecules* **2000**, *33* (22), 8119–8121.
- (20) Pasch, H.; Trathnigg, B. *HPLC of Polymers*; U.S. Government Printing Office: 1999.
- (21) Pasquino, R.; Vasilakopoulos, T. C.; Jeong, Y. C.; Lee, H.; Rogers, S.; Sakellariou, G.; Allgaier, J.; Takano, A.; Brás, A. R.; Chang, T.; Gooßen, S.; Pyckhout-Hintzen, W.; Wischniewski, A.; Hadjichristidis, N.; Richter, D.; Rubinstein, M.; Vlassopoulos, D. Viscosity of Ring Polymer Melts. *ACS Macro Lett.* **2013**, *2* (10), 874–878.
- (22) Doi, Y.; Matsumoto, A.; Inoue, T.; Iwamoto, T.; Takano, A.; Matsushita, Y.; Takahashi, Y.; Watanabe, H. Re-examination of terminal relaxation behavior of high-molecular-weight ring polystyrene melts. *Rheol. Acta* **2017**, *56* (6), 567–581.
- (23) Borger, A.; Wang, W.; O'Connor, T. C.; Ge, T.; Grest, G. S.; Jensen, G. V.; Ahn, J.; Chang, T.; Hassager, O.; Mortensen, K.; Vlassopoulos, D.; Huang, Q. Threading–Unthreading Transition of Linear-Ring Polymer Blends in Extensional Flow. *ACS Macro Lett.* **2020**, *9* (10), 1452–1457.
- (24) Parisi, D.; Ahn, J.; Chang, T.; Vlassopoulos, D.; Rubinstein, M. Stress Relaxation in Symmetric Ring-Linear Polymer Blends at Low Ring Fractions. *Macromolecules* **2020**, *53* (5), 1685–1693.
- (25) McKenna, G. B.; Hadziioannou, G.; Lutz, P.; Hild, G.; Strazielle, C.; Straupe, C.; Rempp, P.; Kovacs, A. J. Dilute solution characterization of cyclic polystyrene molecules and their zero-shear viscosity in the melt. *Macromolecules* **1987**, *20* (3), 498–512.
- (26) Roovers, J. The melt properties of ring polystyrenes. *Macromolecules* **1985**, *18* (6), 1359–1361.
- (27) Roovers, J. Dilute-solution properties of ring polystyrenes. *J. Polym. Sci., Polym. Phys. Ed.* **1985**, *23* (6), 1117–1126.
- (28) Roovers, J. Viscoelastic properties of polybutadiene rings. *Macromolecules* **1988**, *21* (5), 1517–1521.
- (29) Doi, Y. Re-Examination of Terminal Relaxation Behavior for High-Molecular Weight Ring Polystyrenes. In *Ring Polymers: Advances and Perspectives*; Hersonissos Maris Hotel: Crete, Greece, 2017.
- (30) Ge, T.; Panyukov, S.; Rubinstein, M. Self-Similar Conformations and Dynamics in Entangled Melts and Solutions of Nonconcatenated Ring Polymers. *Macromolecules* **2016**, *49* (2), 708–722.
- (31) Rubinstein, M. Dynamics of Ring Polymers in the Presence of Fixed Obstacles. *Phys. Rev. Lett.* **1986**, *57* (24), 3023–3026.
- (32) Halverson, J. D.; Lee, W. B.; Grest, G. S.; Grosberg, A. Y.; Kremer, K. Molecular dynamics simulation study of nonconcatenated ring polymers in a melt. II. Dynamics. *J. Chem. Phys.* **2011**, *134* (20), 204905.
- (33) Tsalikis, D. G.; Alatas, P. V.; Peristeras, L. D.; Mavrantzas, V. G. Scaling Laws for the Conformation and Viscosity of Ring Polymers in

the Crossover Region around Me from Detailed Molecular Dynamics Simulations. *ACS Macro Lett.* **2018**, *7* (8), 916–920.

(34) Obukhov, S.; Johnner, A.; Baschnagel, J.; Meyer, H.; Wittmer, J. P. Melt of polymer rings: The decorated loop model. *EPL (Europhysics Letters)* **2014**, *105* (4), 48005.

(35) Ohta, Y.; Kushida, Y.; Matsushita, Y.; Takano, A. SEC–MALS characterization of cyclization reaction products: Formation of knotted ring polymer. *Polymer* **2009**, *50* (5), 1297–1299.

(36) Ohta, Y.; Nakamura, M.; Matsushita, Y.; Takano, A. Synthesis, separation and characterization of knotted ring polymers. *Polymer* **2012**, *53* (2), 466–470.

(37) Gooßen, S.; Brás, A. R.; Pyckhout-Hintzen, W.; Wischniewski, A.; Richter, D.; Rubinstein, M.; Roovers, J.; Lutz, P. J.; Jeong, Y.; Chang, T.; Vlassopoulos, D. Influence of the Solvent Quality on Ring Polymer Dimensions. *Macromolecules* **2015**, *48* (5), 1598–1605.

(38) Parisi, D.; Kaliva, M.; Costanzo, S.; Huang, Q.; Lutz, P. J.; Ahn, J.; Chang, T.; Rubinstein, M.; Vlassopoulos, D. Nonlinear rheometry of entangled polymeric rings and ring-linear blends. *J. Rheol.* **2021**, *65* (4), 695–711.

(39) Zhou, Y.; Hsiao, K.-W.; Regan, K. E.; Kong, D.; McKenna, G. B.; Robertson-Anderson, R. M.; Schroeder, C. M. Effect of molecular architecture on ring polymer dynamics in semidilute linear polymer solutions. *Nat. Commun.* **2019**, *10* (1), 1753.

(40) Banik, S.; Kong, D.; San Francisco, M. J.; McKenna, G. B. Monodisperse Lambda DNA as a Model to Conventional Polymers: A Concentration-Dependent Scaling of the Rheological Properties. *Macromolecules* **2021**, *54* (18), 8632–8654.

(41) Laib, S.; Robertson, R. M.; Smith, D. E. Preparation and Characterization of a Set of Linear DNA Molecules for Polymer Physics and Rheology Studies. *Macromolecules* **2006**, *39* (12), 4115–4119.

(42) Hays, J. B.; Magar, M. E.; Zimm, B. H. Persistence length of DNA. *Biopolymers* **1969**, *8* (4), 531–536.

(43) Bouchiat, C.; Wang, M. D.; Allemand, J. F.; Strick, T.; Block, S. M.; Croquette, V. Estimating the Persistence Length of a Worm-Like Chain Molecule from Force-Extension Measurements. *Biophys. J.* **1999**, *76* (1), 409–413.

(44) Larson, R. G. The rheology of dilute solutions of flexible polymers: Progress and problems. *J. Rheol.* **2005**, *49*, 1–70.

(45) Heo, Y.; Larson, R. G. The scaling of zero-shear viscosities of semidilute polymer solutions with concentration. *J. Rheol.* **2005**, *49*, 1117–1128.

(46) Liu, Y.; Jun, Y.; Steinberg, V. Concentration dependence of the longest relaxation times of dilute and semi-dilute polymer solutions. *J. Rheol.* **2009**, *53* (5), 1069–1085.

(47) Rendell, R. W.; Ngai, K. L.; McKenna, G. B. Molecular weight and concentration dependences of the terminal relaxation time and viscosity of entangled polymer solutions. *Macromolecules* **1987**, *20* (9), 2250–2256.

(48) Musti, R.; Sikorav, J.-L.; Lairez, D.; Jannink, G.; Adam, M. Viscoelastic properties of entangled DNA solutions. *C. R. Acad. Sci., Ser. IIB: Mec., Phys., Chim., Astron.* **1995**, *320*, 599–605.

(49) Zhou, Y.; Schroeder, C. M. Dynamically Heterogeneous Relaxation of Entangled Polymer Chains. *Phys. Rev. Lett.* **2018**, *120* (26), 267801.

(50) Likhtman, A. E.; McLeish, T. C. B. Quantitative Theory for Linear Dynamics of Linear Entangled Polymers. *Macromolecules* **2002**, *35* (16), 6332–6343.

(51) Robertson, R. M.; Laib, S.; Smith, D. E. Diffusion of isolated DNA molecules: Dependence on length and topology. *Proc. Natl. Acad. Sci. U. S. A.* **2006**, *103* (19), 7310.

(52) Ausubel, F. M. *Short Protocols in Molecular Biology: A Compendium of Methods from Current Protocols in Molecular Biology*, 5th ed.; Wiley: New York, 2002.

(53) Tanyeri, M.; Ranka, M.; Sittipolkul, N.; Schroeder, C. M. A microfluidic-based hydrodynamic trap: design and implementation. *Lab Chip* **2011**, *11* (10), 1786–1794.

(54) Banik, S.; Kong, D.; San Francisco, M. J.; McKenna, G. B. Monodisperse lambda DNA as a model to conventional polymers: A

concentration dependent scaling of the rheological properties. *Macromolecules* **2021**, *54*, 8632.

(55) Li, Y.; Hsiao, K.-W.; Brockman, C. A.; Yates, D. Y.; Robertson-Anderson, R. M.; Kornfield, J. A.; San Francisco, M. J.; Schroeder, C. M.; McKenna, G. B. When Ends Meet: Circular DNA Stretches Differently in Elongational Flows. *Macromolecules* **2015**, *48* (16), 5997–6001.

(56) Klein, J. Dynamics of entangled linear, branched, and cyclic polymers. *Macromolecules* **1986**, *19* (1), 105–118.

(57) Mills, P. J.; Mayer, J. W.; Kramer, E. J.; Hadziioannou, G.; Lutz, P.; Strazielle, C.; Rempp, P.; Kovacs, A. J. Diffusion of polymer rings in linear polymer matrices. *Macromolecules* **1987**, *20* (3), 513–518.

(58) Tsaliakis, D. G.; Mavrantzas, V. G.; Vlassopoulos, D. Analysis of Slow Modes in Ring Polymers: Threading of Rings Controls Long-Time Relaxation. *ACS Macro Lett.* **2016**, *5* (6), 755–760.

(59) Berry, G. C.; Fox, T. G. The viscosity of polymers and their concentrated solutions. *Fortschritte der Hochpolymeren-Forschung* **1968**, *5/3*, 261–357.

(60) Heo, Y.; Larson, R. G. Universal scaling of linear and nonlinear rheological properties of semidilute and concentrated polymer solutions. *Macromolecules* **2008**, *41*, 8903–8915.

(61) Bravo-Anaya, L.; Rinaudo, M.; Martinez, F. Conformation and rheological properties of calf-thymus DNA in solution. *Polymers* **2016**, *8*, 51.

(62) Mason, T. G.; Dhople, A.; Wirtz, D. Linear Viscoelastic Moduli of Concentrated DNA Solutions. *Macromolecules* **1998**, *31* (11), 3600–3603.

(63) Robertson, R. M.; Smith, D. E. Self-Diffusion of Entangled Linear and Circular DNA Molecules: Dependence on Length and Concentration. *Macromolecules* **2007**, *40* (9), 3373–3377.

(64) Michieletto, D.; Turner, M. S. A topologically driven glass in ring polymers. *Proc. Natl. Acad. Sci. U. S. A.* **2016**, *113* (19), 5195.

(65) Lo, W.-C.; Turner, M. S. The topological glass in ring polymers. *EPL (Europhysics Letters)* **2013**, *102* (5), S8005.

(66) Cox, W. P.; Merz, E. H. Correlation of dynamic and steady flow viscosities. *J. Polym. Sci.* **1958**, *28* (118), 619–622.

(67) Soskey, P. R.; Winter, H. H. Large Step Shear Strain Experiments with Parallel-Disk Rotational Rheometers. *J. Rheol.* **1984**, *28* (5), 625–645.

(68) Yan, Z.-C.; Costanzo, S.; Jeong, Y.; Chang, T.; Vlassopoulos, D. Linear and Nonlinear Shear Rheology of a Marginally Entangled Ring Polymer. *Macromolecules* **2016**, *49* (4), 1444–1453.